POLITECNICO DI TORINO
Repository ISTITUZIONALE

Sustainable Photoinduced Frontal Polymerization of Acrylic Resins Reinforced by Biofillers

Original
Sustainable Photoinduced Frontal Polymerization of Acrylic Resins Reinforced by Biofillers / Dizman, H.M., Vitale, A., Bongiovanni, R.. - In: POLYMER COMPOSITES. - ISSN 1548-0569. - ELETTRONICO. - 47:9(2026), pp. 8525-8535. [10.1002/pc.70707]

Availability:
This version is available at: 11583/3016194 since: 2026-10-01T10:04:03Z

Publisher:
John Wiley and Sons

Published
DOI:10.1002/pc.70707

Terms of use:

This article is made available under terms and conditions as specified in the corresponding bibliographic description in the repository

Publisher copyright

(Article begins on next page)

26 November 2026

Check for updates

Polymer Composites

WILEY | spe INSPIRING PLASTICS PROFESSIONALS

RESEARCH ARTICLE OPEN ACCESS

Sustainable Photoinduced Frontal Polymerization of Acrylic Resins Reinforced by Biofillers

Huseyin Mirac Dizman[1] | Alessandra Vitale[1,2] | Roberta Bongiovanni[1,2]

[1]Department of Applied Science and Technology, Politecnico di Torino, Torino, Italy | [2]INSTM – Politecnico di Torino Research Unit, Firenze, Italy

Correspondence: Roberta Bongiovanni (roberta.bongiovanni@polito.it)

Received: 14 July 2025 | **Revised:** 23 October 2025 | **Accepted:** 19 November 2025

Keywords: biobased acrylate | biofiller | composite | photoinduced frontal polymerization | wood adhesive

ABSTRACT

In this study, the synthesis of sustainable biocomposites was successfully achieved using the photo-induced frontal polymerization (PIFP) method, which is highly energy-efficient. A diacrylate containing renewable carbon was selected as a monomer, while a trifunctional acrylate was used as a diluent at different ratios; wood powder and cellulose powder were then added to obtain biocomposites. The maximum amount of wood powder was set at 30 phr by weight, and for cellulose, at 50 phr. In the experiments performed, the effects of the diluent and biofiller amounts on the frontal polymerization velocity, the maximum temperature of the process, and the monomer conversion were investigated. Additionally, depending on the amount of biofillers in the formulation, the photoinitiator, thermal initiator, and light intensity were optimized. Finally, the sample with the highest wood powder content was tested for use as a filler for repairing or joining wooden parts.

1 | Introduction

Frontal polymerization is a polymerization process that can be initiated at a certain point in the system by an external stimulus (e.g., heat, light) and then propagates autonomously, similar to a domino effect. Although it was first discovered in the early 1970s in the Soviet Union by Chechilo and his colleagues [1], most of the research in this field has taken place after its rediscovery in 1991 by Pojman [2].

Frontal polymerization can be categorized into three types depending on the external stimulus used for initiation: thermal-frontal polymerization, photofrontal polymerization, and isothermal frontal polymerization [3]. Additionally, based on whether the system can continue on its own after the removal of the external stimulus, it can be classified as autocatalytic or non-autocatalytic frontal polymerization. In catalytic systems, polymerization continues autonomously after the external stimulus is removed, whereas in non-catalytic systems, the polymerization stops when the stimulus is removed [4, 5]. In this work, the term "photo-induced frontal polymerization" (PIFP) refers specifically to an autocatalytic thermal frontal polymerization where a photoreaction initiates the thermal front.

PIFP stands out due to several advantageous features. Firstly, in PIFP, since the reaction proceeds autonomously once the external stimulus is removed, it is considered energy efficient. Several studies in the literature show that only a few seconds of irradiation are sufficient to initiate frontal polymerization [6–9]. Additionally, compared to conventional photopolymerization systems, PIFP enables the production of much thicker polymers and polymerization in light-hindered areas, making it an attractive method [4, 10].

However, despite these advantages, there are certain limitations that restrict the practical applications of frontal polymerization. For example, PIFP requires highly reactive monomers, limiting its range of applications. Moreover, Pojman and his colleagues demonstrated that acrylate monomers with equivalent weights above 150 do not support PIFP [11].

[Correction added on 28, January 2026, after first online publication: The copyright line was changed.]

This is an open access article under the terms of the Creative Commons Attribution License, which permits use, distribution and reproduction in any medium, provided the original work is properly cited.

© 2025 The Author(s). *Polymer Composites* published by Wiley Periodicals LLC on behalf of Society of Plastics Engineers.

Highlights

- Photo-induced frontal polymerization (PIFP) of biobased monomer was studied
- The effects of different process parameters were analyzed
- Composites with wood and cellulose powder (up 50 phr) were successfully cured
- The application of the composites as a wood adhesive was investigated

In PIFP, in addition to the monomer, the thermal initiator can have a crucial effect on both the kinetics of polymerization and the physical properties of the polymer. Most of the thermal initiators used in frontal polymerization studies are peroxide derivatives, which can lead to the formation of reactive and nonreactive oxygen species and small volatile organic compounds as by-products during decomposition [12, 13]. As a result, bubble formation may occur in the final product, negatively impacting its mechanical properties and causing a heterogeneous structure [14–16].

Apart from the thermal initiator, the high temperatures reached during the PIFP reaction can cause low molecular weight species such as monomers and solvents to boil, leading to bubble formation in the product [17]. Therefore, the use of solvents has been minimized or eliminated; alternatively, high boiling point solvents have been used [18], or efforts have been made to reduce the maximum reaction temperature below the solvent's boiling point [19]. Liska and coauthors published a report on a bubble-free, steady-state thermal front reaction in water, in which a new thermal initiator was synthesized. This initiator minimized gas formation while maintaining suitable reactivity [20].

Additionally, minimizing heat loss from the front to the surroundings is a crucial issue. Front quenching reduces the temperature below the critical level required to maintain self-sustaining frontal polymerization. Moreover, the resulting polymers exhibit uneven properties. From a chemical standpoint, various polymerization processes are affected by unwanted termination reactions or slow background gelation. In radical chain polymerizations, for instance, coupling events decrease the concentration of reactive species that can add monomers in the reaction medium, which in turn slows the observed polymerization rate. Reactor boundary conditions determine the extent of heat loss in the frontal polymerization process. For instance, thermally insulated reaction vessels dissipate heat more slowly than those made of conductive materials, helping to maintain a consistent temperature within the reaction medium. The ratio of effective volume to exposed surface area (i.e., at the reactor boundary) and the shape of the reactor are crucial factors in heat loss [21–26].

Once the chemical and physical phenomena associated with frontal polymerization are well understood, PIFP represents a low-energy alternative for synthesizing both thermoset polymers and moldable thermoplastics. Moreover, it enables a variety of advanced applications, such as the fabrication of porous and gradient materials, the incorporation of high filler loadings, and effective curing in regions inaccessible or impractical for traditional photoprocesses [27, 28].

This study investigates the use of PIFP to cure thick, biobased acrylic monomer samples, including those located in light-restricted areas. The effects of incorporating natural fillers such as wood and cellulose powder were also explored to evaluate the potential of these systems for material consolidation, that is, their application in adhesives, repairs, and sealants.

Additionally, process optimization was examined with respect to thermal effects, frontal velocity, monomer conversion, reaction mechanisms, formulation types, and environmental as well as processing conditions.

2 | Experimental

2.1 | Materials

1,10-Decanediol diacrylate (DDDA), with a minimum biorenewable carbon content of 60%, and the thermal initiator dilauroyl peroxide (Luperox LP) were kindly donated by Arkema. Ethyl phenyl(2,4,6-trimethylbenzoyl) phosphinate photoinitiator (TPO-L) was kindly provided by IGM Resins Italia Srl and trimethylolpropane triacrylate (TMPTA) was purchased from Sigma-Aldrich. The chemical structure of the products is shown in Figure 1a. Lignobest C200 wood powder (from Holzmühle Westerkamp GmbH Visbek, Germany; particle size below 125 μm) and TECHNOCELL FM8 cellulose powder (8–12 μm) produced from FSC-certified European wood, were used as filler. Fillers were dried in the oven at 150°C for 2 h before they were used. NEUKASIL RTV 10 silicone was purchased from Altropol Kunststoff GmbH and used to prepare molds.

2.2 | Photoinduced Frontal Polymerization Procedure

Different amounts of acrylates (DDDA and TMPTA) were mixed with LP (thermal initiator) at a concentration in the range 0.2%–2% by weight, and ArgoLab AU-32 ultrasonic bath was used until the thermal initiator was completely dissolved in the acrylate mixture. Following this step, TPO-L (photoinitiator) at a concentration in the range 1%–2% by weight was added to the solution and stirred until the solution became homogeneous.

To prepare the composites, dried wood powder or cellulose powder was added in varying amounts, up to 50 phr, to the freshly prepared monomer mixtures. The mixtures were then manually stirred until a uniform dispersion was achieved.

A negative mold was 3D printed using the Anycubic Photon Mono X to prepare silicone molds. Subsequently, a mixture of silicone and crosslinker was poured into the negative mold and allowed to cure at room temperature for 24 h. After curing, the solid silicone was removed from the negative mold and the freshly prepared formulations were poured into silicone molds

15480569, 2026, 9, Downloaded from https://4spepublications.onlinelibrary.wiley.com/doi/10.1002/pc.70707 by Politecnico Di Torino Sist. Bibl Del Polit Di Torino, Wiley Online Library on [01/10/2026]. See the Terms and Conditions (https://onlinelibrary.wiley.com/terms-and-conditions) on Wiley Online Library for rules of use; OA articles are governed by the applicable Creative Commons License

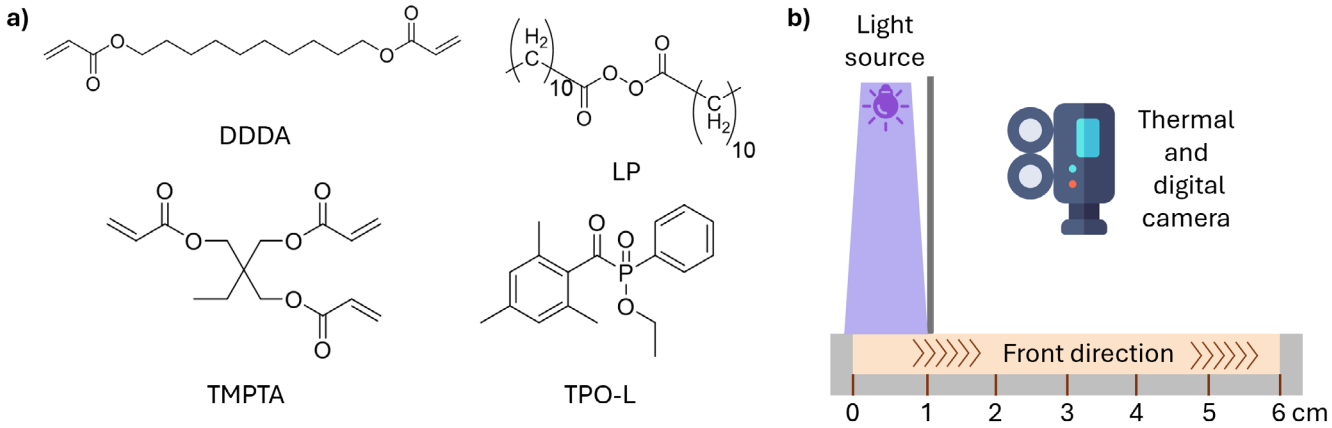

FIGURE 1 | (a) Chemical structure of the products used and (b) PIFP experimental setup.

(length: 60 mm, width: 10 mm, depth: 1, 3, 4, and 5 mm). In some cases, a 2.5 mm thick glass plate was used to cover the formulations, to minimize heat loss caused by the low amount of thermal initiator and to ensure uniform polymer thickness.

The HAMAMATSU LC8 lighting unit, equipped with a medium-pressure mercury light source, was used in all experiments with varying light intensity, ranging from 20 to 200 mW/cm^2 (UVA) depending on the formulation. An optical fiber was used to irradiate a 1 cm^2 area on the surface of the mold from above for 30 s. The frontal propagation was monitored using a FLIR E6-XT thermal camera and a digital camera (see Figure 1b). Frontal velocity was determined by using the time elapsed between the initial and final positions, based on video footage recorded with the digital camera.

2.3 | Monomer Conversion

A Fourier Transform Infrared (FTIR) spectrometer (Thermo Fisher Scientific Nicolet iS50), in attenuated total reflectance (ATR) mode, with a spectral range of 4000–400 cm^{-1}, was used to analyze the polymerized samples. After the polymerization was complete, samples with a length of 60 mm were marked using a ruler: the first point was placed 5 mm from the mold edge, and the remaining points were marked at 10 mm intervals thereafter. Then, cuts were made at these marked lines using a small saw, and the polymer powder released during the cutting process was collected and analyzed by FTIR. The spectral region between 3000 and 2880 cm^{-1} (CH_2) was chosen as the reference band, and the area between 1645 and 1630 cm^{-1} (C═C) was used to calculate the conversion. Each measurement was repeated three times. The equation used to calculate the conversion is given in Equation (1).

Degree of conversion:

$$\text{Conversion}\,(\%) = 100\,x\left(1 - \frac{\left(\frac{A_{1645\ \text{cm}^{-1}}}{A_{3000\ \text{cm}^{-1}}}\right)_{\text{CURED}}}{\left(\frac{A_{1645\ \text{cm}^{-1}}}{A_{3000\ \text{cm}^{-1}}}\right)_{\text{UNCURED}}}\right) \quad (1)$$

2.4 | Polymers and Composites Characterization

Differential scanning calorimetry (DSC) measurements were carried out by means of a Netzsch DSC 204 F1 Phoenix in the temperature range from 20°C to 250°C at a heating and cooling rate of 10°C min^{-1} under a nitrogen flux. A heat–cool–heat procedure was performed.

Viscosity measurements were performed using an Anton Paar MCR702e Rheometer at room temperature. Parallel plate geometry with a 25 mm diameter (PP25-LPP25/TD) was used to test the samples. The gap between the plates was set to 0.3 mm.

The ZEISS Merlin field emission scanning electron microscope (FE-SEM) was used to analyze the morphology of the samples. For sample preparation, the samples were first placed in liquid nitrogen for a few seconds and then broken (brittle fracture) by hand. Afterwards, platinum (Pt) coating of the samples was performed using a Quorum Q150T ES sputter coater, and FE-SEM analysis was conducted on the cross-sections of the samples.

Sample made of DDDA and TMPTA (70:30 w/w ratio) and containing 30 phr of wood powder was tested as an adhesive for wood. Specimens were prepared as follows: a *Swietenia mahogany* wood piece was shaped to form the mold (Figure S10); the wooden pieces were placed on an aluminum foil with a 10 mm gap between them, which was filled with the freshly prepared formulation. The sample was then irradiated from the upper left using a light intensity of 200 mW/cm^2. After polymerization, pull tests in tension were performed using an Instron 3366 electromechanical universal testing machine equipped with a 500 N load cell, at a speed of 10 mm min^{-1}.

3 | Results and Discussion

3.1 | Frontal Polymerization of Biosourced Acrylates

Photo-induced frontal polymerization of the biosourced difunctional acrylate DDDA was carried out in silicone molds, which, due to their thermal insulating properties, minimize heat loss that could otherwise hinder or even quench the propagating front, whose progression relies on thermal diffusion [29, 30]. Preliminary experiments were conducted under various conditions, including changes in initiator concentration, light intensity and resin volume, as well as testing in air or under inert atmosphere, with or without a glass cover.

15480569, 2026, 9, Downloaded from https://4spepublications.onlinelibrary.wiley.com/doi/10.1002/pc.70707 by Politecnico Di Torino Sist. Bibl Del Polit Di Torino, Wiley Online Library on [01/10/2026]. See the Terms and Conditions (https://onlinelibrary.wiley.com/terms-and-conditions) on Wiley Online Library for rules of use; OA articles are governed by the applicable Creative Commons License

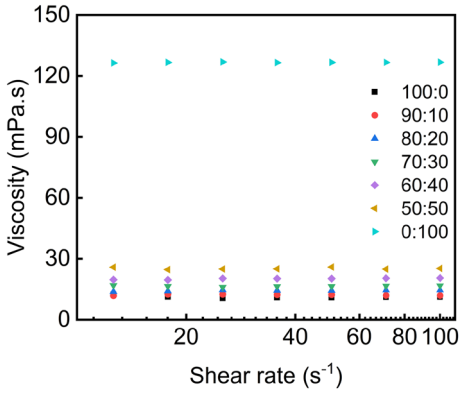

FIGURE 2 | Viscosity values for the formulations with different DDDA:TMPTA ratio (w/w).

TABLE 1 | Effect of sample thickness on PIFP.

Sample composition: DDDA:TMPTA ratio (w/w)	Mold depth—Sample thickness			
	5 mm	4 mm	3 mm	1 mm
100:0	X	X	X	X
90:10	X	X	X	X
80:20	✓	X	X	X
70:30	✓	✓	✓	X
60:40	✓	✓	✓	X
50:50	✓	✓	✓	X
0:100	✓	✓	✓	✓

Note: The tick (✓) indicates successful initiation and interrupted propagation of the polymerization front along the full length of the mold; the cross (X) indicates either no initiation or premature termination of the polymerization front. PIFP conditions: LP = 0.3 w%, TPO-L = 1 w%, light intensity = 20 mW/cm^2, irradiation time = 30 s, inert atmosphere.

Table S1 outlines the experimental parameters investigated for the PIFP of DDDA, indicating which conditions resulted in a successful process, that is, the obtaining of samples 60 mm long (front traveling distance was 50 mm being the irradiated zone 10 mm long). A sustainable thermal front was observed when both the photoinitiator and the thermal initiator were used at a concentration of 2 w%. Indeed, during photopolymerization experiments without a glass cover, it was noted that the final specimen was uneven, with non-uniform thickness: monomer accumulated beneath the irradiated area, while the non-irradiated section became progressively thinner. Additionally, the resin overflowed from the mold (Figure S1). Oxygen and light intensity had no significant effect on front propagation under the tested conditions. As clearly shown in Figure S2, bubble formation consistently occurred in the final products when the thermal initiator concentration was 2 w%, an amount necessary to sustain a propagating front along the entire 60 mm length of the mold.

To reduce the amount of thermal initiator required, and thus mitigate bubble formation, the formulation was modified by adding the multifunctional monomer TMPTA, which increased the reactivity of the system. This modification also altered the viscosity, which is known to significantly affect frontal polymerization. Specifically, when viscosity is low, heat loss due to buoyancy and surface tension-driven convection can quench the propagating front, while increasing the viscosity helps minimize heat loss, thereby sustaining front propagation [29, 30]. Formulations containing different ratios of DDDA:TMPTA were investigated, and their viscosity as a function of shear rate is shown in Figure 2. All formulations exhibit Newtonian behavior, characterized by a constant viscosity regardless of the shear rate. The viscosity of pure DDDA is around 13 mPa s and increases by the addition of TMPTA (whose viscosity is around 125 mPa s); when the TMPTA content reaches 50% by weight, the viscosity rises to 25 mPa s (nearly doubling).

PIFP experiments were conducted using mixtures of the two monomers at varying weight ratios, while reducing the thermal initiator concentration to 0.3 w%, as detailed in Table S2. A self-sustained front 60 mm long was successfully achieved with an irradiation time of 30 s at a light intensity of 20 mW/cm^2, when the TMPTA content was ≥ 20 w% and sample thickness ≥ 3 mm.

After fixing the contents of the thermal and photoinitiators, as well as the light intensity and irradiation time, the effect of sample thickness on the frontal polymerization process was investigated. In fact, it is known from the literature that increasing the sample thickness extends the distance between the position of the maximum temperature, typically located at the bottom of the system, and the surface where heat losses occur, thereby reducing the impact of these losses on front dynamics [31, 32]. Table 1 summarizes the results, indicating the conditions that led to a successful PIFP process, with the polymerization front traveling along the full length of the sample.

The results indicate that when the sample thickness is reduced to 1 mm, only the formulation containing neat TMPTA (0:100) was able to successfully polymerize by PIFP (with the front traveling along the full length of the mold, i.e., for 60 mm). Moreover, when the TMPTA content was reduced to 20% by weight (80:20), only the thickest sample (5 mm) supported efficient frontal propagation. In contrast, for the DDDA:TMPTA ratios 50:50, 60:40, and 70:30 formulations, successful frontal polymerization was observed at sample thicknesses of 5, 4, and 3 mm.

Once the 6 cm-long samples were prepared by PIFP, monomer conversion was monitored by FTIR ATR spectroscopy at various distances from the irradiation area for different sample thicknesses. This analysis was performed by sectioning the solid polymer and collecting samples from specific positions, as described in the Experimental part and illustrated in Figure 3a. Representative spectra are presented in Figure S3. The acrylic group conversion was calculated according to Equation (1), monitoring the change in the C=C absorption band in the 1645–1630 cm^{-1} range, and using the 3000–2880 cm^{-1} (CH_2) region as the reference band. The effects of the TMPTA content and of mold depth on monomer conversion were investigated, and are shown in Figure 3.

Considering the effect of the DDDA:TMPTA weight ratio, the conversion is generally comparable across all formulations that support successful frontal polymerization (Figure 3). Formulations containing equal weight fractions of DDDA and

15480569, 2026, 9, Downloaded from https://4spepublications.onlinelibrary.wiley.com/doi/10.1002/pc.70707 by Politecnico Di Torino Sist. Bibl Del Polit Di Torino, Wiley Online Library on [01/10/2026]. See the Terms and Conditions (https://onlinelibrary.wiley.com/terms-and-conditions) on Wiley Online Library for rules of use; OA articles are governed by the applicable Creative Commons License

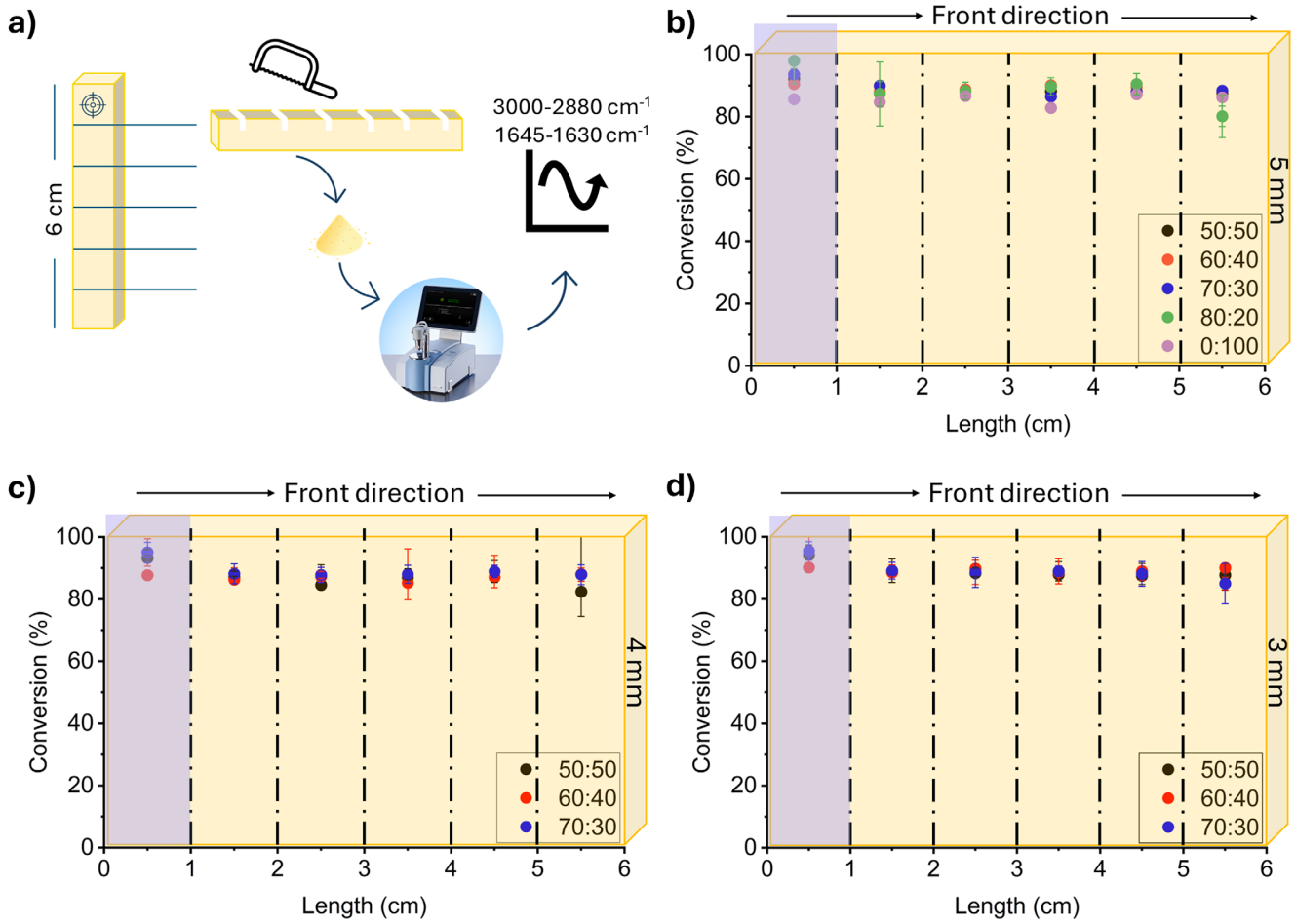

FIGURE 3 | (a) Schematic representation of FT-IR measurements set-up to analyze the monomer conversion in different positions along the sample length. (b–d) Conversion of DDDA:TMPTA formulations with different weight ratios, polymerized by PIFP in molds with a depth of 5 mm (b), 4 mm (c), and 3 mm (d).

TMPTA (50:50) achieved conversions of 88.2% ± 1.2%, regardless of polymer thickness. Similarly, the 60:40 and 70:30 formulations yielded comparable results. For the 80:20 formulation, the monomer conversion in the 5 mm thick specimen was calculated to be 87.2% ± 2.6%. However, in thinner samples, frontal polymerization either failed to initiate upon irradiation or, if initiated, terminated prematurely before completing the reaction; consequently, FT-IR data were not recorded. A similar outcome was observed for the 90:10 and 100:0 formulations, in which no frontal polymerization occurred at any of the thicknesses investigated.

As shown in Figure 3, analysis of monomer conversion along the sample length (i.e., with increasing distance from the initiation point corresponding to the irradiated area) revealed that, in all samples, conversion remained consistently within the 85%–90% range throughout the non-irradiated zone, with no significant variation as distance increased. In contrast, the conversion in the irradiated region was slightly higher, ranging from 90% to 95%.

Since a sample thickness of 5 mm enabled successful PIFP processing of a wider range of formulations, while also maximizing the content of the biosourced monomer DDDA, further characterizations were performed at this thickness. Relevant parameters that ensure the continuity of frontal polymerization are the frontal velocity and the maximum temperature. A particularly important limitation in the application of frontal polymerization is the risk of front extinction, which occurs when heat losses exceed a critical threshold [31].

The balance between heat generation and heat loss is influenced by the reactivity of the monomers and the efficiency of heat transfer between the system and its surroundings. Frontal velocity plays a crucial role in maintaining this balance: generally, a slowdown in frontal velocity prolongs the polymerization time, leading to increased heat dissipation to the environment. Under such conditions, frontal polymerization may initiate but terminate prematurely before the reaction is completed. Figure 4 presents the frontal velocities of the formulations with different DDDA:TMPTA weight ratios, which were calculated using video recordings obtained with a digital camera.

The formulation containing only TMPTA was the fastest, with a frontal velocity of 7.1 ± 0.6 cm min^{-1}. When the TMPTA content was reduced to 50% by weight, the velocity decreased to 4.8 ± 0.3 cm min^{-1}. Subsequently, as the TMPTA ratio continued to decrease, a slowdown in the frontal velocity was observed, and when the TMPTA ratio dropped to 20%, the velocity further declined to 3.6 ± 0.2 cm min^{-1}. However, no significant

15480569, 2026, 9, Downloaded from https://4spepublications.onlinelibrary.wiley.com/doi/10.1002/pc.70707 by Politecnico Di Torino Sist. Bibl Del Polit Di Torino, Wiley Online Library on [01/10/2026]. See the Terms and Conditions (https://onlinelibrary.wiley.com/terms-and-conditions) on Wiley Online Library for rules of use; OA articles are governed by the applicable Creative Commons License

correlation is observed between monomer conversion and frontal velocity (Figure 4).

After PIFP, DSC analyses were performed on samples having 5 mm thickness (the thermal curves are collected in Figure S4). All systems are fully amorphous, as expected. No discernible thermal transitions, including the glass transition, were observed up to 250°C, in agreement with the literature [33–35].

3.2 | Frontal Polymerization of Composites

Two types of biofillers (i.e., wood powder and cellulose powder) were incorporated into the reactive formulations to prepare sustainable composites via PIFP, and the effects of filler type and loading on the polymerization process were investigated.

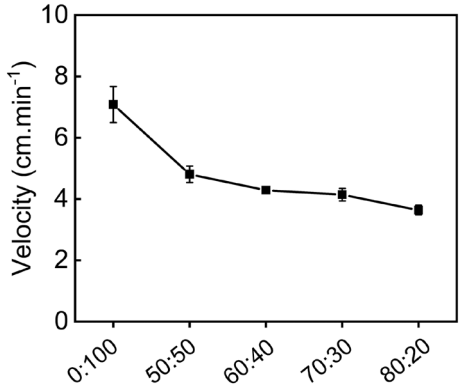

FIGURE 4 | Monomer conversion and frontal velocity of formulations with varying DDDA:TMPTA ratios by weight.

Preparation of composites based on pure DDDA was attempted; however, the front could not be sustained (see Table S3 and Figure S5). Despite the use of high amounts of thermal initiator (2 w%), the reaction of pure DDDA was ineffective in sustaining the front, and when a high filler content (30 phr of wood powder) was used, the frontal process did not even start. As a result, TMPTA was incorporated into the system, and the DDDA:TMPTA 70:30 monomer composition was selected due to its high monomer conversion and relatively high bio-based acrylate content. However, at high filler loadings (30 phr of wood powder or 50 phr of cellulose powder), the process conditions optimized for the neat polymer system (0.3 w% LP, 1 w% TPO-L, irradiation under 20 mW/cm^2 light intensity, as described above) failed to initiate frontal polymerization. Consequently, the processing parameters had to be adjusted to accommodate the presence of fillers.

There are various reasons for the lowering of reactivity upon addition of fillers. The first factor is the increase in viscosity of the reactive formulations (Figure S6). Moreover, the interaction between the light and fillers can affect the photopolymerization kinetics. In the presence of fillers, light can be absorbed by the filler and/or scattering can occur depending on the type of filler. As a result of these interactions, insufficient photoinitiator may be excited by the light, causing the reaction to proceed slowly or not initiate at all. To address this issue, the amount of photoinitiator and/or light intensity can be increased. Another important factor is the filler's ability to absorb heat released

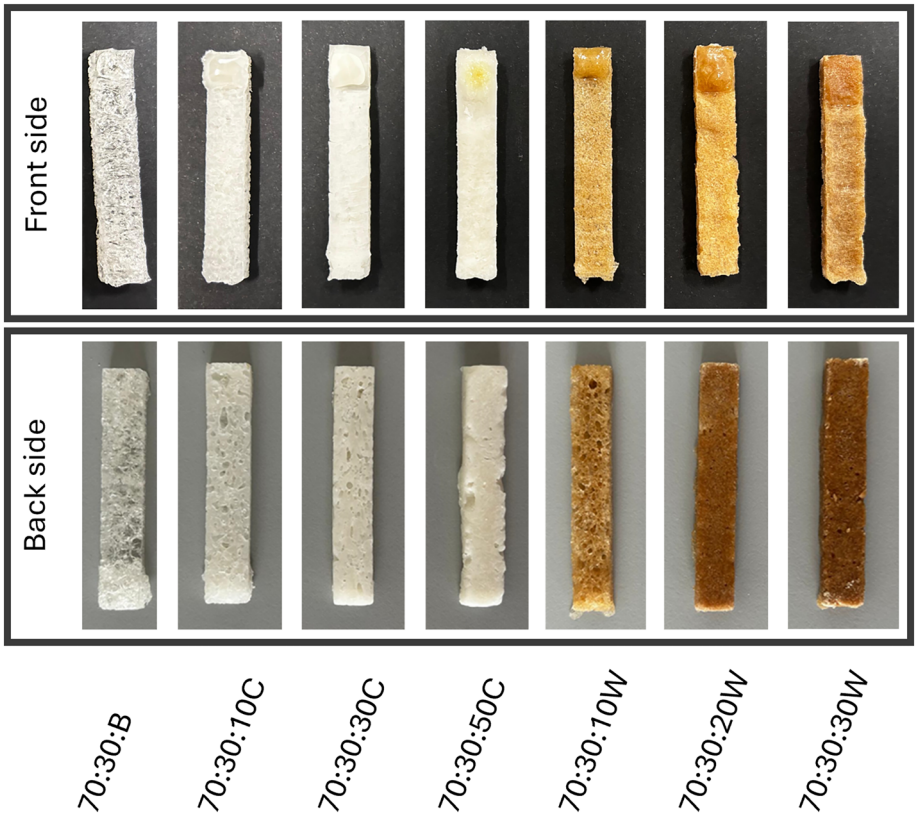

FIGURE 5 | Photos of the polymerized composite samples containing biofiller at different loading (DDDA:TMPTA weight ratio 70:30, B = blank W = wood powder, C = cellulose powder).

15480569, 2026, 9, Downloaded from https://4spepublications.onlinelibrary.wiley.com/doi/10.1002/pc.70707 by Politecnico Di Torino Sist. Bibl Del Polit Di Torino, Wiley Online Library on [01/10/2026]. See the Terms and Conditions (https://onlinelibrary.wiley.com/terms-and-conditions) on Wiley Online Library for rules of use; OA articles are governed by the applicable Creative Commons License

during polymerization. In such cases, the available heat may be insufficient to initiate frontal polymerization or may cause the front, once initiated, to terminate prematurely. To address this issue, the amount of thermal initiator in the formulation can be increased.

Therefore, herein, the concentrations of both LP and TPO-L in the 70:30 monomer system were increased to 2 w%; the reference sample is labeled 70:30:B, and all subsequent formulations containing filler were prepared using these initiator concentrations. Moreover, the light dose was adjusted based on the type and content of filler. Wood powder (W) was added at 10, 20 and 30 phr, while the cellulose powder (C) content was 10, 30 and 50 phr. The composition of the tested formulations as well as the experimental conditions employed for the PIFP process are presented in detail in Table S4. In all reported conditions, the frontal polymerization was successful: photographs taken from the front and back parts of the composites obtained after polymerization are presented in Figure 5. Frontal polymerization of selected formulations is shown in Videos S1 and S2.

The morphology of the composite samples was studied by electron microscopy. Figure 6 presents FE-SEM images of the cross-sections of samples containing biofillers and reveals that cellulose powder is homogeneously distributed throughout the polymer matrix. In contrast, wood powder exhibits a more heterogeneous distribution, and the presence of micropores within the matrix is also evident.

The monomer conversion of the biocomposite samples were estimated by FTIR-ATR (spectra are reported in Figure S7). The results (Figure 7) depended on both the type and amount of filler. The conversion of the sample without biofiller was found to be 89.5% ± 2.6%, and similar values were obtained with the inclusion of 10, 30, and 50 phr of cellulose powder. The conversion values for samples containing 10, 20, and 30 phr of wood powder were calculated as 89.9% ± 1.7%, 87.6% ± 0.4%, and 87.9% ± 1.1%, respectively (Figure 7b). These results indicate that the addition of cellulose or wood powder to the system, regardless of the amount, does not have a significant effect on monomer conversion.

It should be noted that if the fillers are not dried before use, the water content in the powder markedly influences the degree of conversion (a comparison between the 70:30:10W samples with and without filler drying is provided in Figure S8). Without the drying treatment, that is, without removing residual water from the biofiller, the monomer conversion is lower and the polymerization process is less efficient.

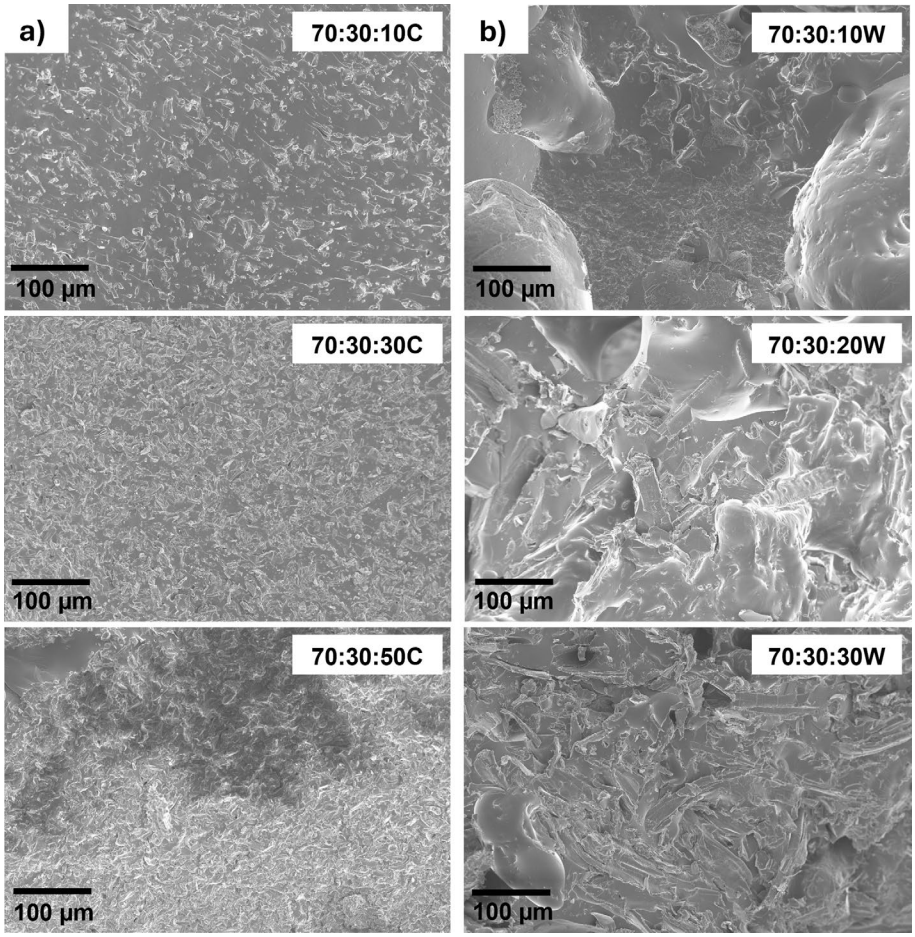

FIGURE 6 | Cross-sectional FE-SEM images of the samples obtained by loading different amounts of bio-filler into the 70:30 DDDA:TMPTA sample by weight. Column (a) corresponds to samples containing varying amounts of cellulose powder, while column (b) corresponds to samples containing varying amounts of wood powder.

15480569, 2026, 9, Downloaded from https://4spepublications.onlinelibrary.wiley.com/doi/10.1002/pc.70707 by Politecnico Di Torino Sist. Bibl Del Polit Di Torino, Wiley Online Library on [01/10/2026]. See the Terms and Conditions (https://onlinelibrary.wiley.com/terms-and-conditions) on Wiley Online Library for rules of use; OA articles are governed by the applicable Creative Commons License

DSC analyses showed that no significant change is observed in the presence of biofillers: the curves have no clear glass transition up to 250°C. (Figure S9). For all the systems containing biofillers, the front velocity during PIFP was evaluated, and the results are shown in Figure 7c. In general, the frontal velocity decreases with increasing filler content, as expected. A comparative analysis of the effects of wood powder and cellulose powder on frontal velocity, specifically in samples containing 10 phr of filler, clearly shows that the decrease in frontal velocity is more pronounced in the sample with wood powder than in the one containing the same amount of cellulose powder. These findings highlight the importance of not only the filler type but also particle size and total volume in determining frontal velocity. Further investigation is currently underway to better understand the underlying reasons for these differences.

In addition, when comparing cellulose and wood powder in terms of chemical composition, it is important to note that while wood is primarily composed of cellulose, it also contains lignin and phenolic compounds. These phenolic compounds may act as radical scavengers, potentially quenching some of the radicals generated during polymerization [36]. This could result in a reduction in the frontal polymerization rate. However, since this topic is out of scope for this study, no detailed work on this matter has been conducted.

Maximum temperatures during PIFP were recorded using a thermal camera (see Video S3). Figure 8 reports the evolution of the maximum temperature in the non-irradiated area with time (the test lasted 30 s, independently on the length of the frontally cured samples). The reference 70:30 sample, which contained no fillers, reached a maximum temperature of 257°C approximately 5–6 s after the onset of irradiation, then the maximum temperature remained almost constant for the rest of the process. With the inclusion of cellulose powder, the maximum temperature decreased proportionally with increasing biofiller content. Additionally, the presence of the biofiller caused a slower rise to the maximum temperature. At a cellulose content of 50 phr by weight, the maximum temperature dropped to approximately 195°C and was reached after about 30 s. Upon the addition of wood powder to the system, a similar trend was obtained (Figure 8): a decrease in maximum temperature was observed with increasing filler content, and the time required to reach peak temperature increased. When the wood powder content reached 30 phr, the maximum temperature was reduced to 195°C.

Moreover, analysis of the relationship between frontal velocity and maximum temperature revealed a direct correlation between the two parameters, as expected: increasing biofiller content led to a corresponding decrease in both frontal velocity and maximum temperature.

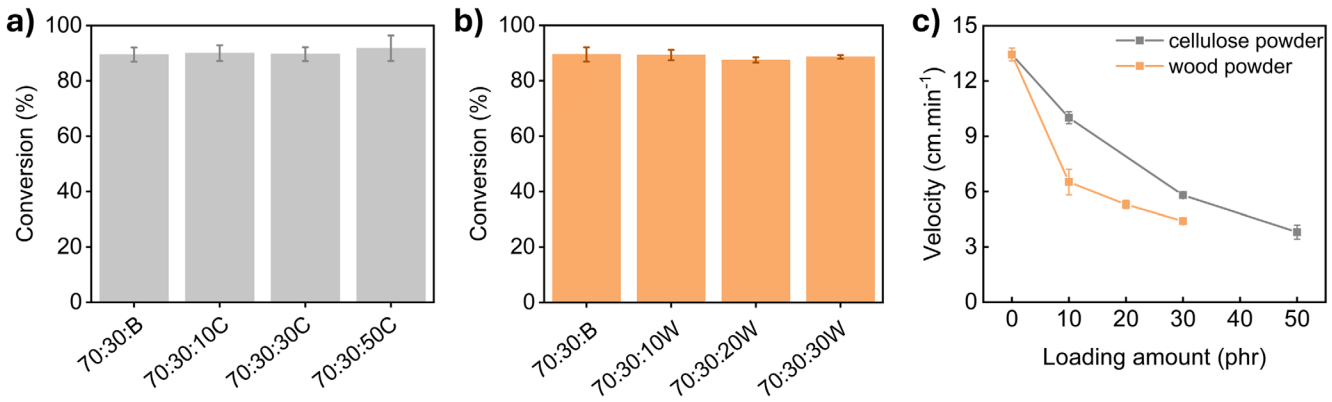

FIGURE 7 | (a) Monomer conversions of samples containing different amounts of cellulose powder, (b) samples containing different amounts of wood powder, and (c) comparison of frontal velocities for samples containing either cellulose or wood powder (reference sample = 70:30B, W = wood powder, C = cellulose powder).

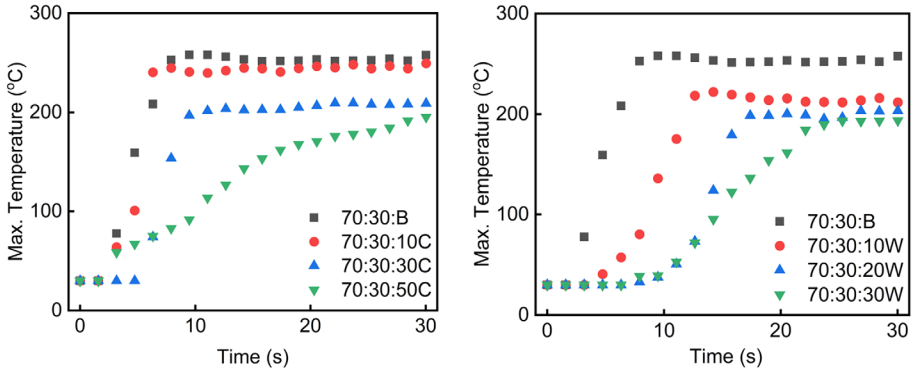

FIGURE 8 | Time-dependent maximum temperature profiles recorded during PIFP of systems containing different biofillers (DDDA:TMPTA weight ratio 70:30, B = blank, which is the sample that contains no fillers and is used as a reference; W = wood powder; C = cellulose powder).

15480569, 2026, 9, Downloaded from https://4spepublications.onlinelibrary.wiley.com/doi/10.1002/pc.70707 by Politecnico Di Torino Sist. Bibl Del Polit Di Torino, Wiley Online Library on [01/10/2026]. See the Terms and Conditions (https://onlinelibrary.wiley.com/terms-and-conditions) on Wiley Online Library for rules of use; OA articles are governed by the applicable Creative Commons License

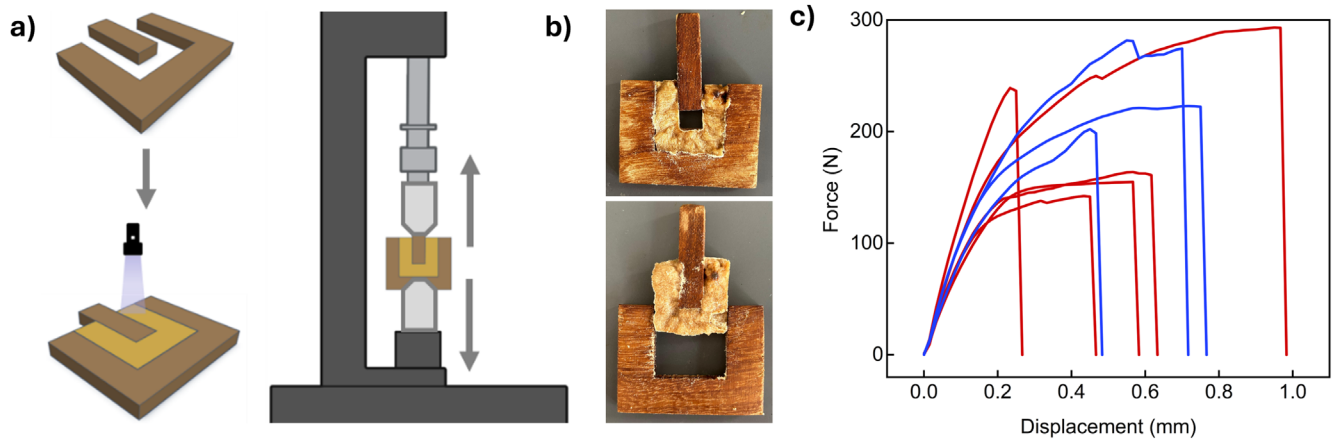

FIGURE 9 | Sketch of (a) the irradiation of the formulation to initiate PIFP, and pull test to assess the adhesion of the composite, (b) pictures of two specimen after adhesive test (upper one represents specimens whose failure takes place at the smaller interface, bottom one represents specimens whose failure takes place at the larger interface). (c) Force versus displacement curves for the 70:30:30 W samples (blue lines refer to specimens whose failure takes place at the smaller interface; red lines refer to specimens whose failure takes place at the larger interface).

3.3 | Use of PIFP for Repair/Join Wooden Parts

As a proof of concept, we demonstrated the applicability of the developed composites as sustainable materials for repairing wooden parts or joining wooden components. In particular, the 70:30:30W formulation was selected due to its higher viscosity, which improved processability, and its higher wood powder content, which enhanced sustainability. The formulation was placed into a wooden mold, and polymerization was initiated from a small lateral point using light at an intensity of 200 mW/cm^2 (Figure 9a). The front propagated throughout the entire material, resulting in a fully crosslinked composite. The polymerized sample was then subjected to a pull test, and the results were recorded.

During the tests all samples showed a load–displacement behavior characterized by an initial elastic region, followed by a plastic region (Figure 9c). The initial slopes in the elastic regions represent the stiffness of the adhesive joints: the average value out of eight trials is 995 ± 137 N/m. After the elastic response, in the plastic region the fracture takes place with a remarkable variability in the maximum force probably due to defects in the joint structure. Out of the eight samples tested, five detached from the larger wooden interface as shown in Figure 9b, bottom picture (red lines in Figure 9c), and the average maximum stress is calculates as 4 ± 1 kPa; while the remaining three detached from the smaller wooden interface as shown in Figure 9b, upper picture (blue lines in Figure 9c), giving an average maximum stress around 9 ± 1.5 kPa.

4 | Conclusion

In this study, the curing of the bio-based acrylic monomers using photoinduced frontal polymerization was successfully achieved obtaining bulk samples in minutes. The reaction could proceed autonomously once the light stimulus is removed, depending on the average functionality of the system (i.e., the amount of acrylic reactive groups) and on the thermal control over the reactive system (e.g., type of mold), given that the right concentration of photoinitiator and thermal initiator is chosen, Suitable conditions also allowed the polymerization process in the presence of wood powder and cellulose powder added at a concentration of up to 30 and 50 phr, respectively: it was found that the addition of bio-based fillers generally led to a decrease in the system's maximum temperature and frontal speed; however, there was no significant difference in monomer conversion.

The composites are proposed as material for repairing or joining wood parts: it was demonstrated that using frontal polymerization quantitative curing of the system was obtained between non-transparent wood joints and the mechanical testing results were satisfactory.

Author Contributions

Huseyin Mirac Dizman: writing – original draft, conceptualization, methodology, data curation, investigation, visualization. **Alessandra Vitale:** writing – review and editing, conceptualization, formal analysis, supervision. **Roberta Bongiovanni:** funding acquisition, writing – review and editing, project administration, resources, supervision, validation, conceptualization, formal analysis.

Acknowledgments

The research work was performed at Politecnico di Torino (POLITO, Italy) within the #horizoneurope20212027 programme under the Marie Skłodowska-Curie Doctoral Networks (MSCA-DN) grant agreement No 101073432. Funding was provided by the European Union.

Funding

This work was supported by EU Horizon 2021 programme MSCA-DN Grant Agreement no. 101073432. Funding was provided by the European Union.

Conflicts of Interest

The authors declare no conflicts of interest.

15480569, 2026, 9, Downloaded from https://4spepublications.onlinelibrary.wiley.com/doi/10.1002/pc.70707 by Politecnico Di Torino Sist. Bibl Del Polit Di Torino, Wiley Online Library on [01/10/2026]. See the Terms and Conditions (https://onlinelibrary.wiley.com/terms-and-conditions) on Wiley Online Library for rules of use; OA articles are governed by the applicable Creative Commons License

Data Availability Statement

The data that support the findings of this study are available from the corresponding author upon reasonable request.

References

1. B. B. Khanukaev, M. A. Kozhushner, N. S. Enikolopyan, and N. M. Chechilo, "Theory of the Propagation of a Polymerization Front," *Combustion Explosion and Shock Waves* 10 (1974): 17–21, https://doi.org/10.1007/BF01463779.

2. J. A. Pojman, "Travelling Fronts of Methacrylic Acid Polymerization," *Journal of the American Chemical Society* 113 (1991): 6284–6286, https://doi.org/10.1021/ja00016a063.

3. Q. Li, H. X. Shen, C. Liu, C. F. Wang, L. Zhu, and S. Chen, "Advances in Frontal Polymerization Strategy: From Fundamentals to Applications," *Progress in Polymer Science* 127 (2022): 101514, https://doi.org/10.1016/j.progpolymsci.2022.101514.

4. F. Petko, A. Świeży, and J. Ortyl, "Photoinitiating Systems and Kinetics of Frontal Photopolymerization Processes-The Prospects for Efficient Preparation of Composites and Thick 3D Structures," *Polymer Chemistry* 12, no. 32 (2021): 4593–4612, https://doi.org/10.1039/d1py00596k.

5. J. T. Cabral, S. D. Hudson, C. Harrison, and J. F. Douglas, "Frontal Photopolymerization for Microfluidic Applications," *Langmuir* 20, no. 23 (2004): 10020–10029, https://doi.org/10.1021/la049501e.

6. J. Sun, L. Zhou, P. Han, and G. Qiao, "UV-Initiated Frontal Polymerization for the Fast Synthesis of Bubble-Free, Self-Propagating Hydrogel Anticorrosive Coatings," *ACS Applied Materials & Interfaces* 15, no. 23 (2023): 28618–28625, https://doi.org/10.1021/acsami.3c04870.

7. J. Staal, B. Caglar, and V. Michaud, "Self-Catalysed Frontal Polymerisation Enables Fast and Low-Energy Processing of Fibre Reinforced Polymer Composites," *Composites Science and Technology* 251 (2024): 110584, https://doi.org/10.1016/j.compscitech.2024.110584.

8. T. Luo, K. Fu, H. Zhu, Y. Chen, B. Yang, and Y. Li, "In-Plane and In-Depth Frontal Polymerization Behaviors of Continuous Fiber-Reinforced Epoxy Composites," *Polymer Composites* 45, no. 4 (2024): 3604–3616, https://doi.org/10.1002/pc.28013.

9. J. A. Dagu Daguerre-Bradford, P. Lepcio, D. S. Camarda, et al., "High Performance Foams and Their Nanocomposites Generated via Liquid State Frontal Polymerization," *Journal of Polymer Science* 62 (2024): 3765–3777, https://doi.org/10.1002/pol.20230167.

10. S. M. Schissel and J. L. P. Jessop, "Transferable Shadow Cure: A New Approach to Achieving Cationic Photopolymerization in Light-Restricted Areas," *Journal of Applied Polymer Science* 139, no. 27 (2022): 52491, https://doi.org/10.1002/app.52491.

11. C. Nason, T. Roper, C. Hoyle, and J. A. Pojman, "UV-Induced Frontal Polymerization of Multifunctional (Meth)acrylates," *Macromolecules* 38, no. 13 (2005): 5506–5512, https://doi.org/10.1021/ma048569y.

12. J. C. Bevington and B. J. Hunt, "The Use of Stabilized Radicals With Monomers and Lauroyl Peroxide," *European Polymer Journal* 40 (2004): 103–108, https://doi.org/10.1016/j.eurpolymj.2003.09.007.

13. X. Zang, L. Jia-Yu, and S. Chi-Min, "Thermal Stability of Lauroyl Peroxide by Isoconversional Kinetics Evaluation and Finite Element Analysis," *Journal of the Taiwan Institute of Chemical Engineers* 45, no. 2 (2014): 461–467, https://doi.org/10.1016/j.jtice.2013.06.004.

14. J. Masere, Y. Chekanov, J. R. Warren, et al., "Gas-Free Initiators for High-Temperature Free-Radical Polymerization," *Journal of Polymer Science Part A: Polymer Chemistry* 38, no. 21 (2000): 3984–3990, https://doi.org/10.1002/1099-0518(20001101)38:21<3984::AID-POLA160>3.0.CO;2-Z.

15. H. Yu, Y. Fang, L. Chen, and S. Chen, "Investigation of Redox Initiators for Free Radical Frontal Polymerization," *Polymer International* 58, no. 8 (2009): 851–857, https://doi.org/10.1002/pi.2590.

16. I. D. Robertson, H. L. Hernandez, S. R. White, and J. S. Moore, "Rapid Stiffening of a Microfluidic Endoskeleton via Frontal Polymerization," *ACS Applied Materials & Interfaces* 6, no. 21 (2014): 18469–18474, https://doi.org/10.1021/am5061596.

17. J. D. Mota-Morales, M. C. Gutiérrez, M. L. Ferrer, et al., "Deep Eutectic Solvents as Both Active Fillers and Monomers for Frontal Polymerization," *Journal of Polymer Science Part A: Polymer Chemistry* 51, no. 8 (2013): 1767–1773, https://doi.org/10.1002/pola.26555.

18. X. Cai, S. Chen, and L. Chen, "Solvent-Free Free-Radical Frontal Polymerization: A New Approach to Quickly Synthesize Poly(N-Vinylpyrrolidone)," *Journal of Polymer Science Part A: Polymer Chemistry* 46, no. 6 (2008): 2177–2185, https://doi.org/10.1002/pola.22552.

19. J. A. Pojman, G. Curtis, and V. M. Ilyashenko, "Frontal Polymerization in Solution," *Journal of the American Chemical Society* 118, no. 15 (1996): 3783–3784, https://doi.org/10.1021/ja9600688.

20. P. M. Potzmann, F. J. Lopez Villanueva, and R. Liska, "UV-Initiated Bubble-Free Frontal Polymerization in Aqueous Conditions," *Macromolecules* 48, no. 24 (2015): 8738–8745, https://doi.org/10.1021/acs.macromol.5b02348.

21. T. Topkaya, Y. Gao, and P. H. Geubelle, "Frontal Polymerization in Short-Fiber-Reinforced Thermoset Composites," *ACS Applied Polymer Materials* 4, no. 10 (2022): 6880–6886, https://doi.org/10.1021/acsapm.2c00818.

22. P. Datta, K. Efimenko, and J. Genzer, "The Effect of Confinement on Thermal Frontal Polymerization," *Polymer Chemistry* 3, no. 12 (2012): 3243–3246, https://doi.org/10.1039/c2py20640d.

23. Q. Z. Yan, W. F. Zhang, G. D. Lu, X. T. Su, and C. C. Ge, "Frontal Polymerization Synthesis of Starch-Grafted Hydrogels: Effect of Temperature and Tube Size on Propagating Front and Properties of Hydrogels," *Chemistry - A European Journal* 12, no. 12 (2006): 3303–3309, https://doi.org/10.1002/chem.200500970.

24. J. A. Pojman, J. Masere, E. Petretto, et al., "The Effect of Reactor Geometry on Frontal Polymerization Spin Modes," *Chaos* 12, no. 1 (2002): 56–65, https://doi.org/10.1063/1.1445436.

25. J. A. Pojman, R. Craven, A. Khan, and W. West, "Convective Instabilities in Traveling Fronts of Addition Polymerization," *Journal of the American Chemical Society* 96, no. 18 (1992): 7466–7472, https://doi.org/10.1021/j100197a062.

26. I. D. Robertson, M. Yourdkhani, P. J. Centellas, et al., "Rapid Energy-Efficient Manufacturing of Polymers and Composites via Frontal Polymerization," *Nature* 557, no. 7704 (2018): 223–227, https://doi.org/10.1038/s41586-018-0054-x.

27. Y. A. Chekanov and J. A. Pojman, "Preparation of Functionally Gradient Materials via Frontal Polymerization," *Journal of Applied Polymer Science* 78, no. 13 (2000): 2398–2404, https://doi.org/10.1002/1097-4628(20001220)78:13<2398::AID-APP170>3.0.CO;2-K.

28. A. D. Tran, T. Koch, P. Knaack, and R. Liska, "Radical Induced Cationic Frontal Polymerization for Preparation of Epoxy Composites," *Composites. Part A, Applied Science and Manufacturing* 132 (2020): 105855, https://doi.org/10.1016/j.compositesa.2020.105855.

29. V. Viner and G. Viner, "Effect of Filler Choice on a Binary Frontal Polymerization System," *Journal of Physical Chemistry. B* 115, no. 21 (2011): 6862–6867, https://doi.org/10.1021/jp112365a.

30. T. Holt, K. Fazende, E. Jee, Q. Wu, and J. A. Pojman, "Cure-On-Demand Wood Adhesive Based on the Frontal Polymerization of Acrylates," *Journal of Applied Polymer Science* 133, no. 40 (2016): 44064, https://doi.org/10.1002/app.44064.

31. Y. Gao, L. E. Rodriguez Koett, J. Hemmer, et al., "Frontal Polymerization of Thin Layers on a Thermally Insulating Substrate," *ACS Applied Polymer Materials* 4, no. 7 (2022): 4919–4927, https://doi.org/10.1021/acsapm.2c00497.

15480569, 2026, 9, Downloaded from https://4spepublications.onlinelibrary.wiley.com/doi/10.1002/pc.70707 by Politecnico Di Torino Sist. Bibl Del Polit Di Torino, Wiley Online Library on [01/10/2026]. See the Terms and Conditions (https://onlinelibrary.wiley.com/terms-and-conditions) on Wiley Online Library for rules of use; OA articles are governed by the applicable Creative Commons License

32. R. Tiani, J. A. Pojman, and L. Rongy, "Critical Role of Layer Thickness in Frontal Polymerization," *Journal of Physical Chemistry. B* 126, no. 19 (2022): 3607–3618, https://doi.org/10.1021/acs.jpcb.2c01252.

33. A. Goswami, G. Srivastava, A. M. Umarji, and G. Madras, "Thermal Degradation Kinetics of Poly(Trimethylol Propane Triacrylate)/poly(Hexane Diol Diacrylate) Interpenetrating Polymer Network," *Thermochimica Acta* 547 (2012): 53–61, https://doi.org/10.1016/j.tca.2012.08.006.

34. P. D. Drumhellere and J. A. Hubbell, "Densely Crosslinked Polymer Networks of Poly(Ethylene Glycol) in Trimethyolpropane Triacrylate for Cell-Adhesion-Resistant Surfaces," *Journal of Biomedical Materials Research* 29 (1995): 207–215, https://doi.org/10.1002/jbm.820290211.

35. K. S. Anseth, C. N. Bowman, and N. A. Peppas, "Dynamic Mechanical Studies of the Glass Transition Temperature of Photopolymerized Multifunctional Acrylates," *Polymer Bulletin* 31 (1993): 229–233, https://doi.org/10.1007/BF00329970.

36. Q. Liu, H. Zhang, H. Ren, and H. Zhai, "Structural Analysis of Light-Colored Separated Lignin (Lignocresol) and Its Antioxidant Properties," *International Journal of Biological Macromolecules* 197 (2022): 169–178, https://doi.org/10.1016/j.ijbiomac.2021.12.144.

Supporting Information

Additional supporting information can be found online in the Supporting Information section. **Data S1:** Supporting Information. **Video S1:** Photoinduced Frontal Polymerization in the presence of 30 phr of cellulose powder (sample 70:30 30C). **Video S2:** Photoinduced Frontal Polymerization in the presence of 30 phr of wood powder (sample 70:30 30W). **Video S3:** Photoinduced Frontal Polymerization monitored by a thermal camera (sample 70:30 30W).

15480569, 2026, 9, Downloaded from https://4spepublications.onlinelibrary.wiley.com/doi/10.1002/pc.70707 by Politecnico Di Torino Sist. Bibl Del Polit Di Torino, Wiley Online Library on [01/10/2026]. See the Terms and Conditions (https://onlinelibrary.wiley.com/terms-and-conditions) on Wiley Online Library for rules of use; OA articles are governed by the applicable Creative Commons License